*Zygote*

**cambridge.org/zyg**

# Histological, histochemical, immunohistochemical and ultrastructural characterization of the testes of the dove

Fatma El-Zahraa A. Mustafa and Ruwaida Elhanbaly

Department of Anatomy and Histology, Faculty of Veterinary Medicine, Assiut University, Egypt

## Research Article

**Cite this article:** Mustafa FEA and Elhanbaly R. (2021) Histological, histochemical, immunohistochemical and ultrastructural characterization of the testes of the dove. *Zygote*. **29**: 33–41. doi: 10.1017/S0967199420000477

Received: 7 May 2020
Accepted: 28 June 2020
First published online: 3 September 2020

**Keywords:**
Androgen; Germ cells; Leydig cell; Myoid cell; Sertoli cells; Telocyte

**Author for correspondence:**
Fatma El-Zahraa A. Mustafa, Department of Anatomy and Histology, Faculty of Veterinary Medicine, Assiut University, 71526, Egypt.
E-mail: f.histology@aun.edu.eg; f.331986@yahoo.com

## Summary

Avian testes have been used in the study of germ cell transfer, importantly for understanding the preservation and control of birds. For this purpose, we use light microscopy, electron microscopy and immunohistochemistry to understand the reproductive efficiency of dove testes. The tunica albuginea was thin and septula testes were not observed. The testicular parenchyma was formed mainly of closely packed convoluted seminiferous tubules with little interstitial area. Three types of spermatogonia were distinguished. The primary spermatocyte appeared as the largest spermatogenic cell and was identified at different stages of meiosis. Different morphological stages of the spermatid were categorized. Various cellular associations were described within the seminiferous epithelium. The cytoplasm of Sertoli cells was pale and ill defined due to its close relationship to the germinal epithelium. The spermatid attached to the luminal border of Sertoli cells and germ cells were closely associated. A single layer of myoid cells surrounded the seminiferous tubule. Testicular telocytes of doves were located in the peritubular region and near the blood vessels. Telopods appeared as long cytoplasmic processes arising from the cell body. Leydig cells were distributed singly or in small groups and cords. The intensity of androgen receptor (AR) immunostaining in the testes of the dove was established for the first time and is described in this paper.

## Introduction

Laughing dove (LD; *Spilopelia senegalensis*) is classified in the family Columbidaes and is found in South Africa (Madkour and Mohamed, 2019). Few previous studies have recorded the reproduction of birds in southern Africa. The LD is a nonseasonal breeder and testes were examined throughout the all year breeding season (Earlé and Dean, 1981).

Testes are formed mainly of two components, the first being the stroma, which mainly forms the capsule and interstitial connective tissue. No septula testes have been observed in bird testes. The second component of the testes is the parenchyma, which forms the seminiferous tubules and interstitial cells. Seminiferous tubules contain Sertoli cells and germ cells.

Meiosis in males is observed only in the testes, which have two major functions, exocrine (sperm production) and endocrine (androgen production) (Lan *et al.*, 2011). During spermatogenesis, the spermatogonia differentiate into sperm. Spermatogonia divide to form primary spermatocytes, which divide to form secondary spermatocytes, and then spermatids change into sperm. Different stages of spermatids are observed during this change. Cytoplasmic bridges connect many germ cells to facilitate the transport of cytoplasmic constituents between cells (Ventela *et al.*, 2003) and progress continuously toward the lumen. The testicular capsule plays an important role in the mechanism of sperm pushing forward (Dharani *et al.*, 2017).

Bird spermatogenesis waves are difficult to distinguished due to their cellular association in small areas within the seminiferous tubule and it has been very difficult to describe for bird testes (Kirby and Froman, 2000).

Different important somatic cells are observed in the testes, inside seminiferous tubules, such as Sertoli cells, and outside the seminiferous tubules, such as myoid cells, Leydig cells and telocytes. Sertoli cells support germ cell development physically and metabolically (Sharpe *et al.*, 2003). Myoid cells are smooth muscle-like cells that help in the transport of spermatozoa (Kormano and Hovatta, 1972). Leydig cells are located within the interstitial connective tissue between seminiferous tubules. Leydig cells are the main source of male sex hormones (Li *et al.*, 2016). Telocytes are widespread interstitial cells observed in the testes of humans (Marini *et al.*, 2018), rabbits (Awad and Ghanem, 2018), and Chinese soft-shelled turtles (Yang *et al.*, 2015), but no previous study has recorded telocytes in the testes of birds.

Androgen is essential for development of the male reproductive system and regulation of spermatogenesis. Androgen performs its function by binding to the androgen receptor (AR; Welsh *et al.*, 2012). Positive immunostaining for the AR in human testes, germ cells, Sertoli cells, and Leydig cells (Vornberger *et al.*, 1994) has been recorded. Testosterone levels



CAMBRIDGE UNIVERSITY PRESS

are controlled by a feedback mechanism through the AR and its loss leads to incomplete meiosis (Holdcraft and Braun, 2004).

Avian testes are important in the study of germ cell transfer (Trefil *et al.*, 2006) and for studies on preservation and control. Previous studies have been made on the testes of chicken (De Reviers *et al.*, 1971), Japanese quail (Lin and Jones, 1992), and turkey (Bakst *et al.*, 2007), but little information is known about dove testes. In the current study, we describe the histological, ultrastructure features and androgen expression of dove testes.

## Materials and methods

### Sample collection

Specimens were collected by a local hunter in Assiut governorate, Egypt and samples taken from the testes of five healthy LD (*Spilopelia senegalensis*). Testes were dissected immediately after slaughtering and fixed in Bouin's fluid.

### Histological examination

The fixed specimens were dehydrated in ethyl alcohol, then cleared with methyl benzoate, and embedded in paraffin wax. Samples were cut at 3–6 µm thickness and stained with the following stains: Harris haematoxylin and eosin, Crossmon's trichrome or Weigert's elastic (Bancroft *et al.*, 2013).

### For semithin sections and transmission electron microscopy (TEM) preparations

Small samples of testes were preserved by immersion in 3% glutaraldehyde in 0.1 M sodium cacodylate buffer (pH 7.3) for 3 h at 4°C (Karnovsky, 1965). Samples were washed in the same buffer for 2 h, and post-fixed with 1% osmium tetroxide in 0.1 M sodium cacodylate buffer at pH 7.2 for 2 h at room temperature. Next, the specimens were dehydrated in ethyl alcohol, followed by propylene oxide and embedded in Araldite.

Semithin sections were cut at 1-µm thickness using a Richert Ultracuts system (Leica, Germany) and stained with toluidine blue for light microscopy. Ultrathin sections (70 nm) were obtained using an Ultrotom-VRV instrument (LKB, Bromma, Germany) and stained with lead citrate and uranyl acetate (Reynolds, 1963). TEM images were captured on a JEOL-100CXII electron microscope.

### Immunohistochemistry

Immunohistochemical detection of the AR in paraffin sections was prepared based on protocols in Hsu *et al.* (1981) using Androgen Receptor Monoclonal Antibody (AR 441) (catalogue no. MA5-13426). Sections (4 µm) of the testes were dewaxed in xylene, rehydrated in ethanol, and sections were rinsed in PBS pH 7.4 (three times for 5 min each time). The actions of endogenous peroxidase were inhibited by adding 1% hydrogen peroxide at room temperature for 10 min. Sections were washed in PBS (pH 7.4) for 5 min, then positioned in 10 mM sodium citrate buffer (pH6.0) and heated (95–98°C) in a water bath (20 min) and then cooled at room temperature. Slides were rinsed in PBS (pH 7.4). Sections were incubated with primary antibodies (30 min) at room temperature, then washed with PBS (pH of 7.4) for 5 min and then incubated with secondary antibody (10 min) at room temperature. Slides were rinsed in PBS (pH 7.4) followed by incubation with drops of streptavidin–peroxidase complex (Thermo Fisher Scientific, USA) for 10 min at room temperature. Sections were rinsed in PBS (pH 7.4) and then counterstained in Harris haematoxylin, dehydrated, cleared, and mounted using DPX.

### Digital coloured images

Transmission electron micrograph images were coloured carefully using Adobe Photoshop software version 6 to increase the visual contrast between several structures on the same electron micrograph.

## Results

### Light microscopy

Testes were surrounded by thin connective tissue tunica albuginea, formed mainly of collagenous fibres. In addition, elastic fibres were arranged in different directions on the capsule. Abundant longitudinally arranged smooth muscle fibres were distributed on the capsule, especially in the inner part of the tunica albuginea. Septula testes were not observed, so there were no lobules on the dove testes. The limited interstitial connective tissues were made up of collagenous, elastic fibres together with blood and numerous lymph vessels (Fig. 1).

The testicular parenchyma was formed mainly of closely packed convoluted seminiferous tubules with little interstitial area containing interstitial cells. Seminiferous tubules contained two types of cells: spermatogenic cells and Sertoli cells. The different types of spermatogenic cells were spermatogonia, primary spermatocytes, secondary spermatocytes, spermatids and sperms. Spermatogonia were located in close proximity to the basement membrane of the seminiferous tubules. Three types of spermatogonia were distinguished based on cytoplasmic and nuclear morphological characteristics: spermatogonia type A (SpA), spermatogonia type intermediate (SpI), and spermatogonia type B (SpB). SpA were dark, large, rounded or elongated cells with large rounded or oval nuclei that contained one or two distinct nucleoli and mainly dispersed chromatin (Fig. 2A, B). SpI were small, rounded, dark cells with a rounded nucleus that showed distinct nucleoli and finely dispersed chromatin (Fig. 2A). SpB appeared as rounded and small cells with a rounded eccentric nucleus with distinct nucleoli and coarse clumped chromatin attached to the nuclear membrane (Fig. 2A).

Primary spermatocytes were located in the intermediate position within the seminiferous tubules. Primary spermatocytes appeared as the largest spermatogenic cell and were identified at different stages of meiosis (Fig. 2C–E). Secondary spermatocytes were located in a more advanced position towards the lumens of the seminiferous tubules and appeared smaller compared with the primary spermatocytes (Fig. 2F).

Different morphological steps of the spermatid were categorized based on the shapes of spermatid, nucleus and chromatin arrangements into eight steps (spermatid step 1, spermatid step 2, spermatid step 3, spermatid step 4, spermatid step 5, spermatid step 6, spermatid step 7 and spermatid step 8). Spermatid step 1: rounded spermatid with rounded nucleus and distinct nucleolus and coarse spread chromatin (Figs 3A and 4). Spermatid step 2: rounded spermatid with a rounded nucleus with a narrow band of chromatin under the nuclear membrane and distinct nucleolus. Thin filaments of chromatin were connected between the nucleolus and peripheral chromatin (Figs 3A and 4). Spermatid step 3: resampling the previous stage and acrosomic granules were observed (Figs 3B and 4). Spermatid step 4: the most characteristic step were the pear-shaped nuclei of spermatids (Figs 3C and 4). Spermatid step 5: oval spermatid showed an oval lightly stained

https://doi.org/10.1017/S0967199420000477 Published online by Cambridge University Press

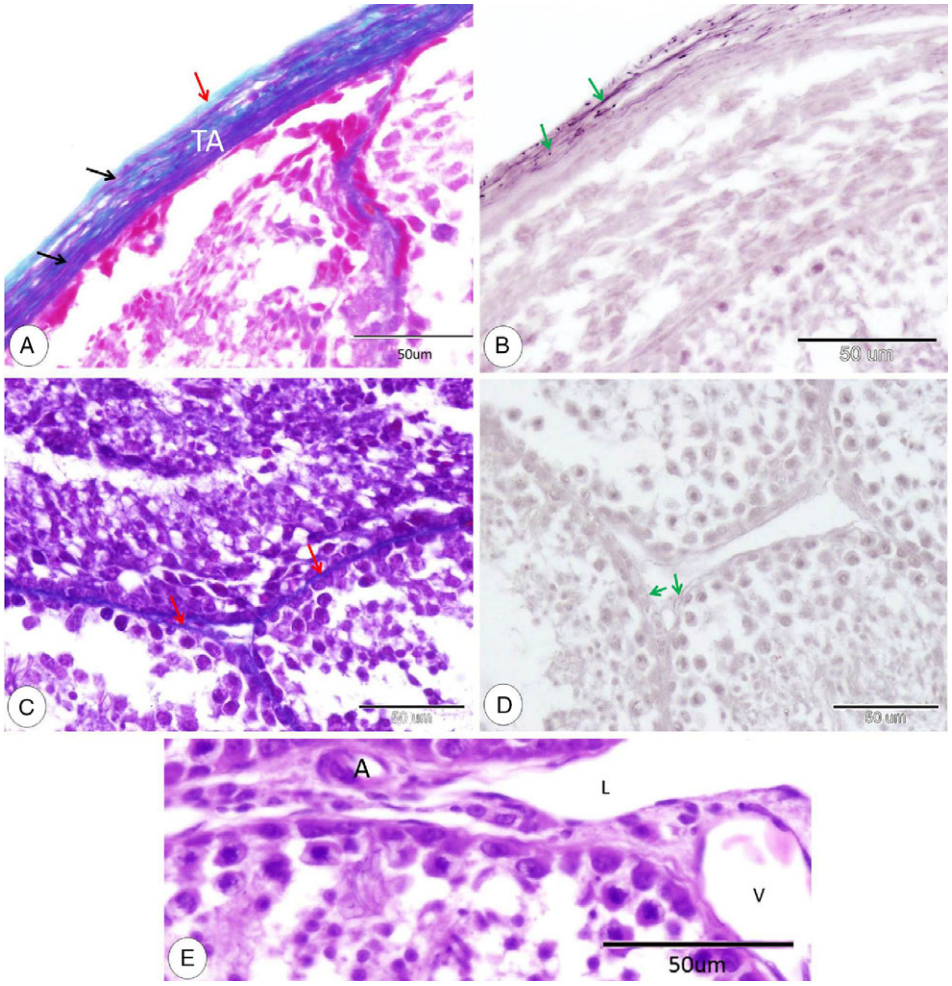


**Figure 1.** General structure of the testicular stroma. (*A*) Tunica albuginea (TA), collagenous fibres (red arrow) and smooth muscle fibres (black arrows) (Crossmon's trichrome). (*B*) Elastic fibres distributed in different direction on tunica albuginea (green arrows) (Weigert's resorcin fuchsin). (*C*) Few interstitial connective tissue contained collagenous connective tissue (red arrows) (Crossmon's trichrome). (*D*) Few elastic fibres on the interstitial connective tissue (green arrows) (Weigert's resorcin fuchsin). (*E*) arteriole (A), venule (V) and lymph vessel (L) on the interstitial connective tissue (HE).

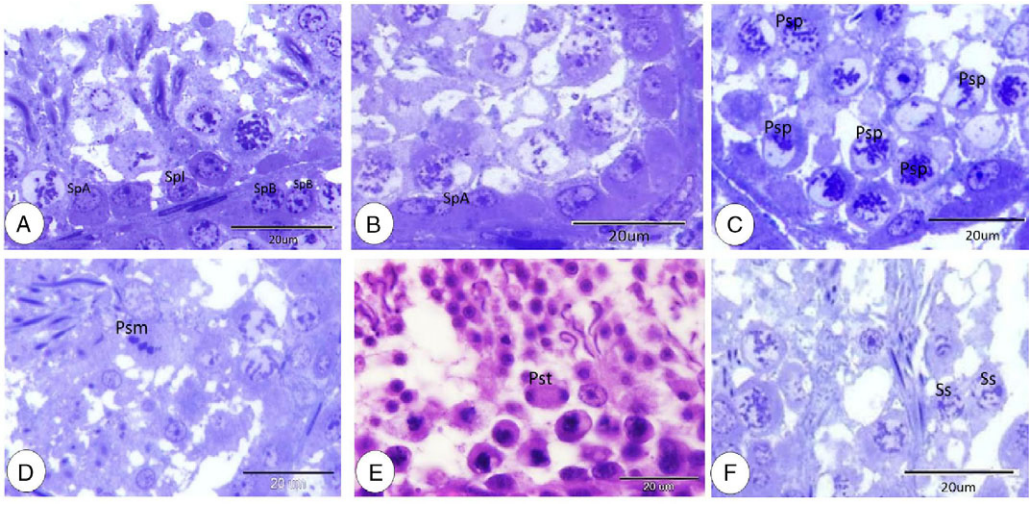


**Figure 2.** Spermatogonia, Primary spermatocyte, and secondary spermatocyte. (*A*, *B*) spermatogonia type A (SpA), spermatogonia type intermediate (SpI) and spermatogonia type B (SpB) (TB). (*C*) Primary spermatocyte at prophase (Psp) (TB). (*D*) Primary spermatocyte at metaphase (Psm) (TB). (*E*) Primary spermatocyte at telophase (Pst) (HE). (*F*) Secondary spermatocyte (Ss) (TB).

nucleus (Figs 3D and 4). Spermatid step 6: the elongated spermatid exhibited elongated more condensed nuclei (Figs 3E and 4). Spermatid step 7: further elongation of spermatids was detected with more elongation and condensation of the nucleus (Figs 3F and 4). Spermatid step 8: the final stage before the release of sperm and consisted of the head with an elongated deeply stained nucleus and a tail (Figs 3G and 4).

Sertoli cell appeared as an elongated large cell with large rounded, lightly stained nuclei with distinct nucleoli. The cytoplasm of Sertoli cells was pale and ill defined due to the close

https://doi.org/10.1017/S0967199420000477 Published online by Cambridge University Press

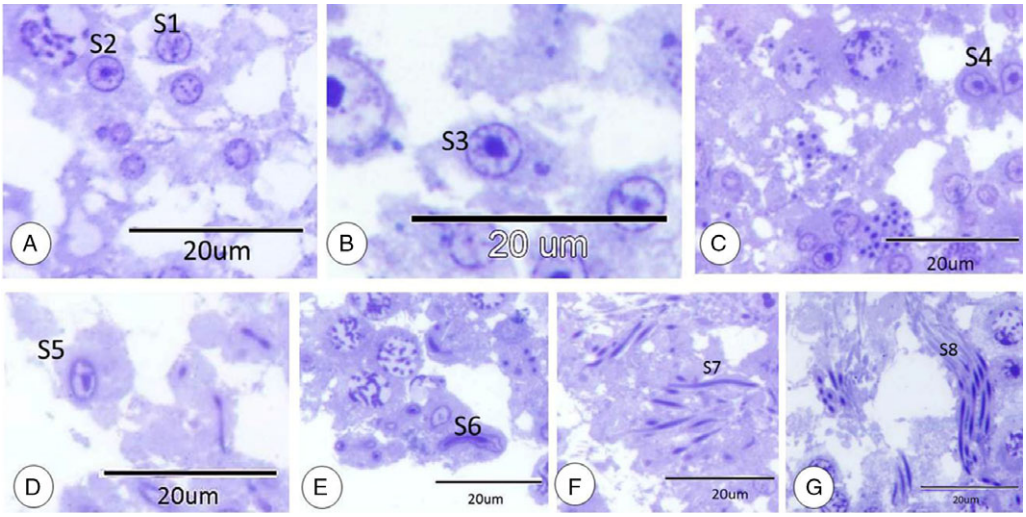


**Figure 3.** Spermatid steps. (*A*) Spermatid step 1(S1) and spermatid step 2 (S2). (*B*) Spermatid step 3 (S3). (*C*) Spermatid step 4 (S4). (*D*) Spermatid step 5 (S5). (*E*) Spermatid step 6 (S6). (*F*) Spermatid step 7 (S7). (*G*) Spermatid step 8 (S8). All stained with TB.

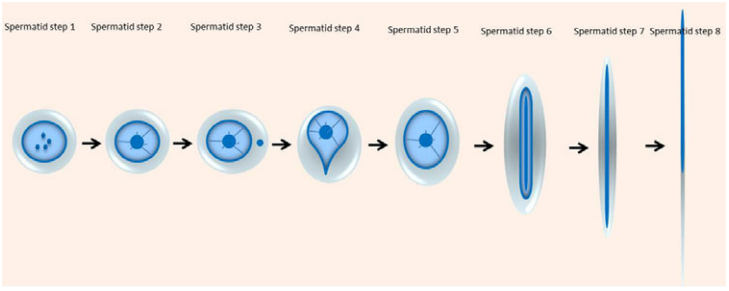


**Figure 4.** Spermatid steps diagram. Spermatid step 1, spermatid step 2, spermatid step 3, spermatid step 4, spermatid step 5, spermatid step 6, spermatid step 7 and spermatid step 8.

association to germinal epithelium. Spermatids were attached to the luminal border of Sertoli cells and germ cells were positioned close to it (Fig. 5A).

Leydig cells could be observed near the blood and lymph vessels in very narrow intertubular spaces. Leydig cells were distributed singly or in small groups and cords. Singly distributed cells were large oval cells with a large oval vesicular nucleus and deeply stained cytoplasm containing lipid droplets (Fig. 5B–D). Cells in groups and cords were fusiform or polyhedral in shape with a pale cytoplasm (Fig. 5C, D). A single layer of myoid cells was surrounded by the seminiferous tubule; the myoid cell was a flat elongated cell with a flat nucleus (Fig. 5B).

Dove testicular telocytes were located in the peritubular region and near blood vessels. Telocytes had a spindle-shaped or triangular-shaped cell body with a large nucleus and small amounts of cytoplasm. Telopods appeared as long cytoplasmic processes arising from the cell body (Fig. 5B, E, F).

Seminiferous epithelium showed seven different cellular associations (stage I, stage II, stage III, stage IV, stage V, stage VI, and stage VII). Each of these were formed from spermatogonia at the basement membrane and at the end at the luminal surface by spermatids. Stage I: spermatogonia arranged close to the basement membrane, then several rows of spermatocytes mainly in the pachytene stage and rounded spermatids were observed at the luminal surface (Fig. 6A). Stage II: different from the previous stage for the primary spermatocytes which becomes zygotene primary spermatocytes (Fig. 6B). Stage III: differs from the previous stages with the presence of spermatocytes at the diplotene stage (Fig. 6B). Stage IV: the main characteristic features of this stage were zygotene and diplotene primary spermatocytes. In addition, spermatids at this stage appeared elongated with elongated nuclei (Fig. 6C). Stage V: at this stage, spermatogonia were observed at the basement membrane, then the pachytene primary spermatocytes were placed at the middle position, and the luminal surface was occupied by more elongated spermatids compared with the previous stage (Fig. 6D). Stage VI: the most obvious features of this stage were the more elongated spermatids with condensed nuclei, which were located at deep positions within Sertoli cells (Fig. 6E). Stage VII: mature stages of spermatid and residual bodies were observed at the luminal border of seminiferous tubules (Fig. 6F).

### *Androgen receptor expression*

The intensity of androgen receptor (AR) immunostaining in dove testes was established for the first time in this study. Spermatogonia had moderate immunostaining for AR in the cytoplasm and slight immunostaining for AR in the nucleus (Fig. 7A). Slight-to-moderate cytoplasmic and nuclear AR immunostaining of the primary spermatocyte was observed (Fig. 7B). Slight-to-moderate cytoplasmic and nuclear AR immunostaining were detected in spermatids (Fig. 7C). Slight-to-moderate immunostaining was detected at the residual body (Fig. 7D). Sertoli cells showed slight immunostaining for the cytoplasm and the nucleus (Fig. 7E). Myoid cells exhibited slight cytoplasmic and nuclear AR immunostaining (Fig. 7F). Moderate cytoplasmic and nuclear AR immunostaining were detected at Leydig cells (Fig. 7G).

### *Ultrastructure*

With a transmission electron microscope, two types of spermatogonia could be distinguished. The first type was characterized by a

https://doi.org/10.1017/S0967199420000477 Published online by Cambridge University Press

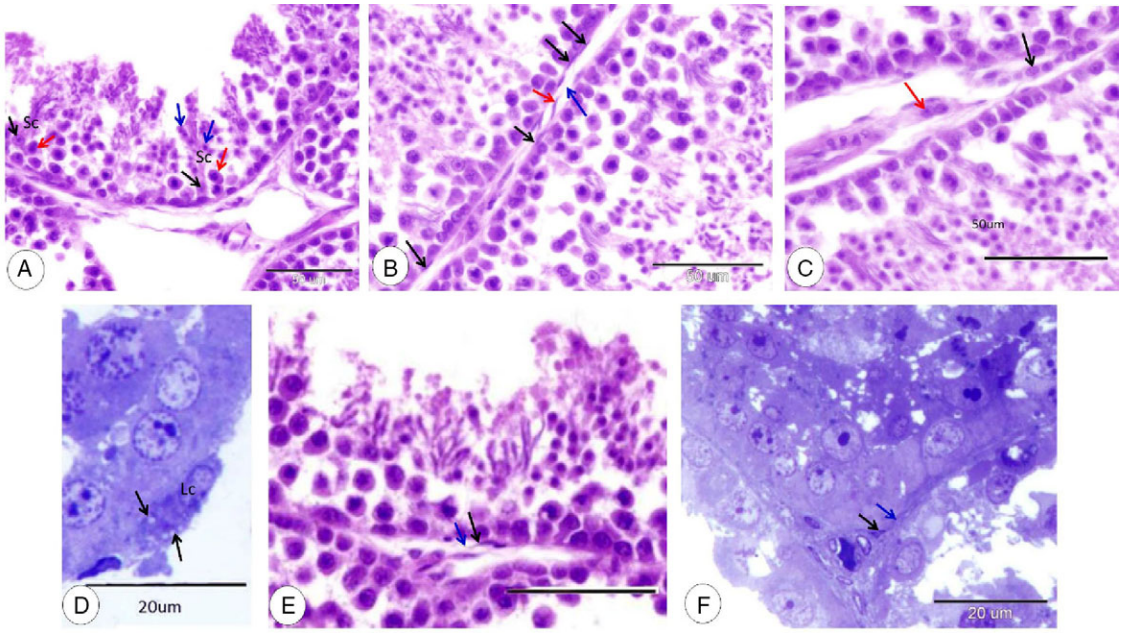


**Figure 5.** Sertoli cell, myoid cells, Leydig cells, and telocytes. (*A*) Sertoli cell (Sc), nucleus of Sertoli cell (black arrows), spermatocyte (red arrow) and spermatid (blue arrow) (HE). (*B*) Myoid cells (black arrows), telocyte (red arrow) and telopodes (blue arrow) (HE). (*C*) Cord of Leydig cells (black arrow) and a small group of Leydig cells (red arrow) (HE). (*D*) Singly distributed Leydig cells (Lc) and lipid droplets (black arrows) (TB). (*E*) Telocyte (black arrow) and telopodes (blue arrow) (HE). (*F*) Telocyte (black arrow) and telopodes (blue arrow) (TB).

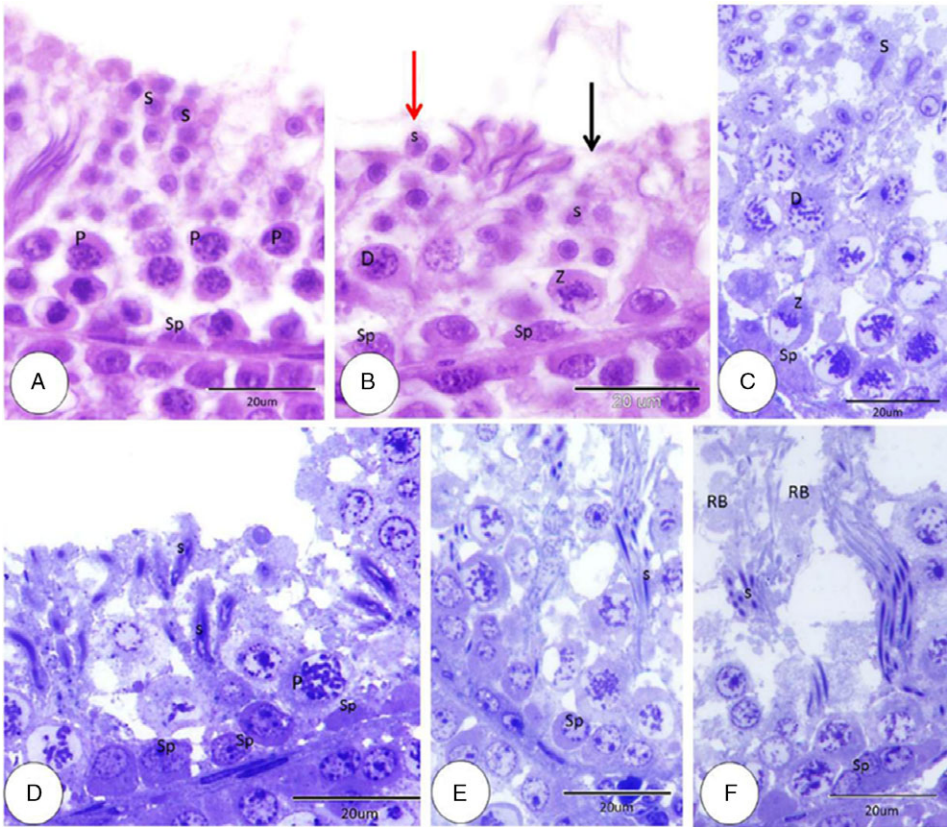


**Figure 6.** Seminiferous epithelium cellular association stages I–VII. (*A*) Stage I: spermatogonia (Sp), pachytene primary spermatocytes (P) and rounded spermatids (S) (HE). (*B*) Stage II (black arrow), stage III (red arrow), spermatogonia (Sp), zygotene primary spermatocytes (Z), diplotene primary spermatocytes (D) and round spermatids (S) (HE). (*C*) Stage IV: spermatogonia (Sp), zygotene primary spermatocytes (Z), diplotene primary spermatocyte (D) and elongated spermatid (S) (HE). (*D*) Stage V: spermatogonia (Sp), pachytene primary spermatocyte (P) elongated spermatid (S) (HE). (*E*) Stage VI: spermatogonia (Sp) and elongated spermatids with condensed nuclei (S) (HE). (*F*) Stage VII: spermatogonia (Sp), mature stage of spermatid (S) and residual body (RB) (HE).

large nucleus with distinct nucleoli, mainly dispersed chromatin and few heterochromatin blocks of different sizes (Fig. 8A). The second type appeared as a rounded cell with a rounded nucleus. Nuclei of spermatogonia showed distinct nucleoli and coarse clumped chromatin attached to the nuclear membrane (Fig. 8B). The cytoplasm of spermatogonia was characterized by well developed rough endoplasmic reticulum, abundant free ribosomes, and numerous mitochondria (Fig. 8C). Primary spermatocytes at

https://doi.org/10.1017/S0967199420000477 Published online by Cambridge University Press

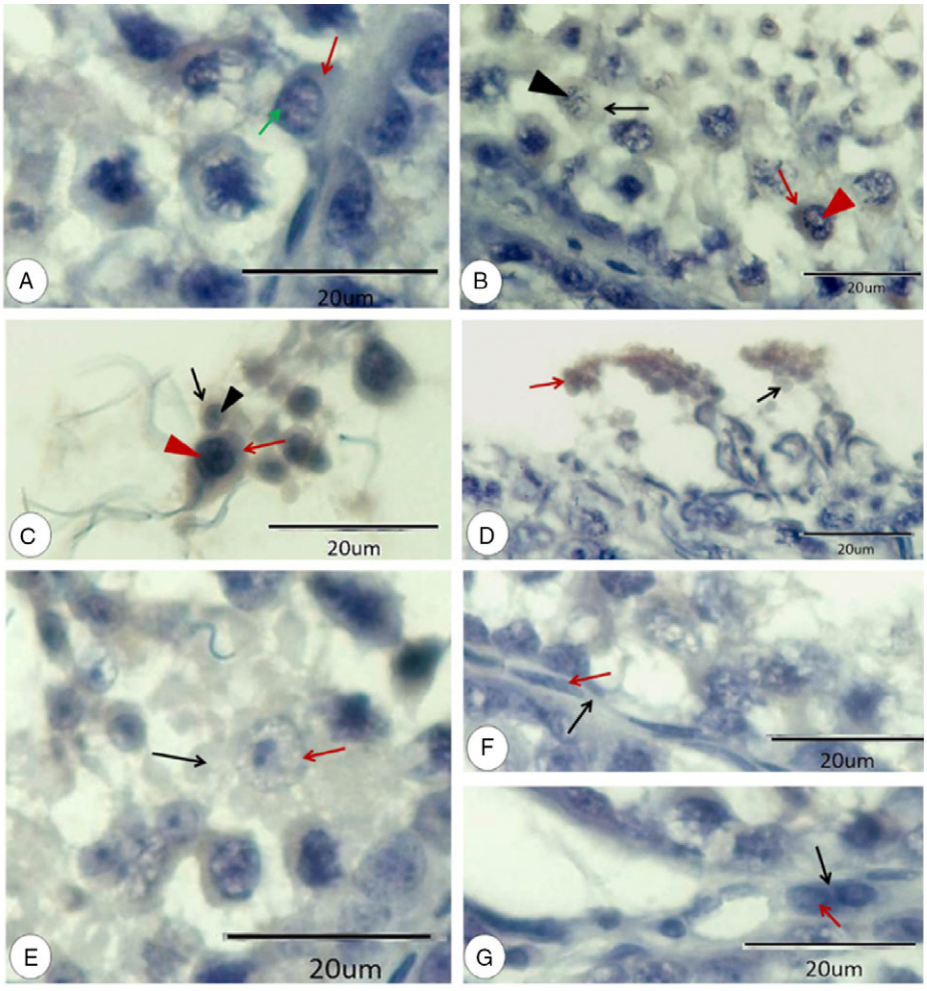


**Figure 7.** Immunohistochemical expression pattern of androgen receptor in the testis of dove. (*A*) Moderate cytoplasmic (red arrow) and slight nuclear (green arrow) immunostaining for AR in the spermatogonia. (*B*) Slight (black arrow) to moderate (red arrow) cytoplasmic and slight (black arrowhead) to moderate (red arrowhead) nuclear AR immunostaining in the primary spermatocyte. (*C*) Slight (black arrow) to moderate (red arrow) cytoplasmic and slight (black arrowhead) to moderate (red arrowhead) nuclear AR immunostaining in spermatid. (*D*) Slight (black arrow) to moderate immunostaining in the residual body (red arrow). (*E*) Slight cytoplasmic (black arrow) and nuclear (red arrow) immunostaining in Sertoli cells. (*F*) Slight cytoplasmic (black arrow) and nuclear (red arrow) AR immunostaining in myoid cells. (*G*) Moderate cytoplasmic (black arrow) and nuclear (red arrow) AR immunostaining in Leydig cells.

prophase were easily distinguished. The cytoplasm of these cells showed abundant mitochondria, free ribosomes and rough endoplasmic reticulum (Fig. 8D).

Rounded spermatids were observed with a rounded nucleus and coarse chromatin attached to the nuclear membrane and distinct nuclei and multiple acrosomal vesicles (Fig. 9A). Single coalesced acrosomal vesicles were observed in another rounded spermatid. Spermatids at this stage showed cytoplasmic bridges (Fig. 9B). In addition, the smaller rounded and oval spermatids demonstrated deeply stained rounded or oval nuclei and vacuolated cytoplasm (Fig. 9C). Elongated spermatids were detected, attached to Sertoli cells and characterized by a deeply stained nucleus and little cytoplasm (Fig. 9D).

Sertoli cells appear as elongated cells with a basal border resting on the basement membrane and apical cytoplasmic processes. The nuclei of Sertoli cells were rounded, pale with fine dispersed chromatin. Spermatids at different stages were attached to the apical border. The cytoplasm contained rough endoplasmic reticulum, numerous mitochondria, and many lysosomes (Fig. 9D).

## Discussion

In the current study, the tunica albuginea of dove testes was found to be thin, and made up of collagen, elastic and reticular fibres. Abundant longitudinally arranged smooth muscle was observed in the dove testicular capsule. Similar findings have been observed for rooster testes by Aire and Ozegbe (2007), who added that smooth muscle fibres of duck tunica albuginea were arranged in longitudinal, transverse and oblique directions. Abundant contractile elements on the bird testicular capsule played an important role in fluid transport.

Our observation did not detect septa on dove testes. In addition, thin layers of interstitial connective tissue were formed, mainly of collagen and elastic fibres. Similar observations have been noted in fowl (Dharani *et al.*, 2017), in quail (Kannan *et al.*, 2008) and in duck (Gerzilov *et al.*, 2016).

In the present study, three types of spermatogonia were observed. Similar findings have been described in turkey (Bakst *et al.*, 2007). In contrast, four types of spermatogonia have been observed in Japanese quail (Lin and Jones, 1992), and five types of spermatogonia have been detected in some mammals (Clermont and Bustos-Obregon, 1968). Spermatogonia divided mitotically during spermatocytogenesis to give primary spermatocytes (Deviche *et al.*, 2011).

In this study, primary spermatocytes were observed at different stages of meiosis. In addition, secondary spermatocytes were observed and located near the luminal border of the seminiferous tubules. Aire (2007) added that primary spermatocyte entered the long prophase of the first maturation division to give secondary spermatocytes. The latter divided quickly to give spermatids.

https://doi.org/10.1017/S0967199420000477 Published online by Cambridge University Press

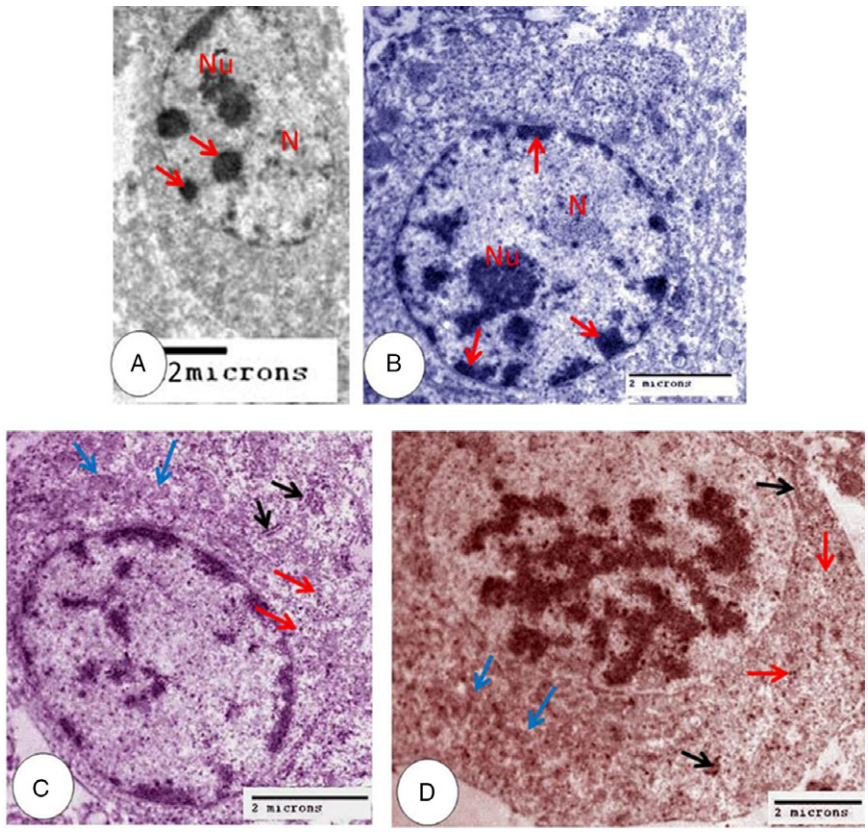


**Figure 8.** Coloured transmission electron microscopy micrograph of spermatogonia and spermatocyte. (*A*) First type spermatogonia nucleus (N), nucleolus (Nu) and heterochromatin blocks (red arrows). (*B*) Second type spermatogonia nucleus (N), nucleolus (Nu) and clumped chromatin (red arrows). (*C*) Spermatogonia characterized by well developed rough endoplasmic reticulum (black arrows), free ribosomes (red arrows) and numerous mitochondria (blue arrows). (*D*) Primary spermatocytes showed abundant mitochondria (blue arrows), free ribosomes (red arrows) and rough endoplasmic reticulum (black arrows).

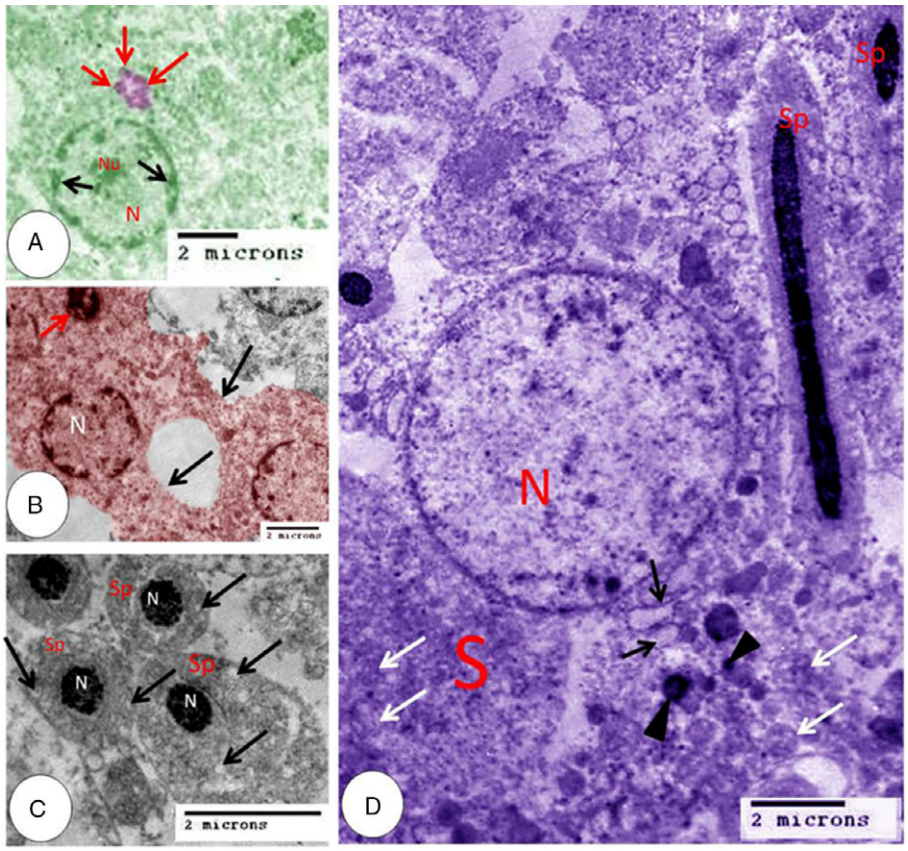


**Figure 9.** Coloured transmission electron microscopy micrograph of spermatid and Sertoli cell. (*A*) Rounded spermatid nucleus (N), nucleolus (Nu), coarse chromatin (black arrows) and multiple acrosomal vesicles (red arrows). (*B*) Rounded spermatid nucleus (N), acrosomal granule (red arrow) and cytoplasmic bridges (black arrows). (*C*) Spermatid (Sp), nucleus (N) and vacuoles (arrows). (*D*) Elongated spermatid (Sp), Sertoli cell (S), nucleus of Sertoli cell (N), rough endoplasmic reticulum (black arrows), mitochondria (white arrows) and lysosomes (black arrowheads).

https://doi.org/10.1017/S0967199420000477 Published online by Cambridge University Press

Spermatids then metamorphosed into sperm during a complex process.

Different stages of spermatid and seven cellular associations could be identified in doves from the present study. Conversely, nine cellular associations have been observed on testes of guinea cock (Abdul-Rahman *et al.*, 2017) and eight cellular associations in guinea fowl (Aire *et al.*, 1980).

In the present study, cytoplasmic bridges were detected between spermatids, this result was supported by Lin and Jones (1992) in quail spermatids. During metamorphosis, spermatid transformed into sperm. Cytoplasmic bridges acted as a molecule exchange pathway to synchronize spermatogenesis (Lin and Jones, 1993; Niedenberger *et al.*, 2018; Villagra *et al.*, 2018).

Several somatic cells were observed within the testes such as Sertoli cells, myoid cells, Leydig cells, and telocytes, but the only somatic cell within the seminiferous tubule was the Sertoli cell. Morphologically, Sertoli cells observed in dove were similar to those in fowl. The close relationship between germ cells and Sertoli cells indicated their role in spermatogenesis and spermiogenesis. Sertoli cells are described as bridge-like cells due to their elongation from the basement membrane to the lumen. This elongation helps in movement of material through the Sertoli cell (Cooksey and Rothwell, 1973). Observation of lipid droplets within Sertoli cells indicated the function of these cells in germ cell nutrition (Shi *et al.*, 2013). Numerous lysosomes in the cytoplasm of Sertoli cells support the phagocytosis of the residual body and degenerating germ cells (Scheltinga and Jamieson, 2003). Based on Villagra *et al.* (2018), lipid in Sertoli cells is said to be raw material for steroid hormones.

Our observation revealed that Leydig cells were distributed singly in small groups or cords and characterized by pale cytoplasm containing lipid droplets, as in mammalian cells. Rothwell (1973) mentioned that fowl Leydig cells were similar to those of mammals. In addition, lipid droplets have been observed in Leydig cells of fowl but not observed in quail (Nicholls and Graham, 1972).

Myoid cells were arranged as a single-cell layer in our study and in rodents (Maekawa *et al.*, 1996). However, multiple layers of myoid cells were observed in the testes of quail (Harrisson and Callebaut, 1993) and fowl (Rothwell and Tingari, 1973). Myoid cells are smooth muscle-like cells and have the contractile ability for sperm and testicular fluid in rodents (Maekawa *et al.*, 1996). The function of myoid cell layers is unclear to date.

We recorded, for the first time, the occurrence of telocytes in the peritubular and perivascular region of dove testes. Our result were in agreement with Marini *et al.* (2018) for human testes. Telocytes have been observed in the peritubular region in mouse testes (Pawlicki *et al.*, 2019) and human testes (Hasirci *et al.*, 2017). Based on Marini *et al.* (2018) testicular telocytes are important players in transporting molecules from outside to inside the tubules and regulating androgen secretion.

Previous studies have described the distribution of AR in mammalian testes in humans (Ruizeveld de Winter *et al.*, 1991), rats (Vornberger *et al.*, 1994), in mice (Wang *et al.*, 2009). No previous study has determined the AR receptor distribution on birds testes. In the current study, we described for the first time AR distribution in dove testes.

In the current study, spermatogonia, primary spermatocytes, spermatids, Sertoli cells, myoid cells and Leydig cells exhibited positive immune staining. Previous studies have detected positive immunostaining for AR in mouse spermatogonia (Zhou *et al.*, 1996), human spermatocytes (Kimura *et al.*, 1993) and rat spermatids (Wright, and Frankel, 1980). Moreover, myoid cells, Sertoli cells and Leydig cells demonstrated positive AR immunostaining (Zhu *et al.*, 2000).

Spermatogenesis is maintained with androgen, which performed its role through the AR (Zhu *et al.*, 2000). In addition, Regadera *et al.* (2001) mentioned that spermatogenesis was dependent on testosterone, which acts through the AR. Based on Holdcraft and Braun (2004), Sertoli cells showed positive immunostaining for the AR. In addition, Sertoli cells regulated meiosis through the AR. Moreover, AR expression was not only detected in other reproductive organs such as epididymis and prostate (Abate-Shen and Shen, 2000), but was expressed in the brain (Sutinen *et al.*, 2017).

In conclusion, light microscopy and electron microscopy studies of dove testes distinguished two types of cells. The first type was germ cells that entered meiosis to produce sperm. Cytoplasmic bridges connected germ cells. Different intensities of immunostaining were expressed on germ cells. The second type was somatic cells such as Sertoli cells, myoid cells, Leydig cells and telocytes, which played important roles in germ cell development.

**Acknowledgements.** This work was supported by the Faculty of Veterinary Medicine, Assiut University, Egypt.

**Conflict of interest.** The authors declare that they have no competing interests.

**Financial support.** The current study has not received any funds from any organizations or institutions.

**Ethical approval and consent to participate.** The study was approved by the Ethics Committee of Assiut University, Egypt.

## References

**Abate-Shen C and Shen MM** (2000). Molecular genetics of prostate cancer. *Genes Dev* **14**, 2410–34.

**Abdul-Rahman II, Obese FY and Robinson JE** (2017). Spermatogenesis and cellular associations in the seminiferous epithelium of Guinea cock (*Numida meleagris*). *Canadian J Anim Sci* **97**, 241–9.

**Aire TA** (2007). Spermatogenesis and testicular cycles. In *Reproductive Biology and Phylogeny of Birds* (ed. Barrie GM Jamieson), CRC Press, pp. 279–348.

**Aire TA and Ozegbe PC** (2007). The testicular capsule and peritubular tissue of birds: morphometry, histology, ultrastructure and immunohistochemistry. *J Anat* **210**, 731–40.

**Aire TA, Olowo-Okorun MO and Ayeni JS** (1980). The seminiferous epithelium in the guinea fowl (*Numida meleagris*). *Cell Tissue Res* **205**, 319–25.

**Awad M and Ghanem ME** (2018). Localization of telocytes in rabbits testis: histological and immunohistochemical approach. *Microsc Res Tech* **81**, 1268–74.

**Bakst MR, Akuffo V, Trefil P and Brillard JP** (2007). Morphological and histochemical characterization of the seminiferous epithelial and Leydig cells of the turkey. *Anim Reprod Sci* **97**, 303–13.

**Bancroft JD, Layton C and Suvarna SK** (2013). *Bancroft's Theory and Practice of Histological Techniques*. Churchill Livingstone, 7th edn.

**Clermont Y and Bustos-Obregon E** (1968). Re-examination of spermatogonial renewal in the rat by means of seminiferous tubules mounted 'in toto'. *Am J Anat* **122**, 237–47.

**Cooksey EJ and Rothwell B** (1973). The ultrastructure of the Sertoli cell and its differentiation in the domestic fowl (*Gallus domesticus*). *J Anat* **114**, 329.

**De Reviers M, Richetin C and Brillard JP** (1971). Le développement testiculaire chez le coq. ii. – morphologie de l'épithélium séminifère et établissement de la spermatogenèse. *Annal Biol Anim Biochim Biophys* **11**, 531–46.

**Deviche P, Hurley LL and Fokidis HB** (2011). Avian testicular structure, function, and regulation. In *Hormones and Reproduction of Vertebrates*. Academic Press, pp. 27–70.

https://doi.org/10.1017/S0967199420000477 Published online by Cambridge University Press

**Dharani P, Kumary SU, Venkatesan S, Joseph C and Geetha R** (2017). Morphometry and histology of the testicular capsule and peritubular tissue of testis of guinea fowl (*Numida meleagris*). *Indian J Vet Anat* **29**, 67–9.

**Earlé RA and Dean WRJ** (1981). Features of spermatogenesis in the laughing dove *Streptopelia senegalensis*. *African Zool* **16**, 109–12.

**Gerzilov V, Bochukov A, Penchev G and Petrov P** (2016). Testicular development in the Muscovy duck (*Cairina moschata*). *Bulg J Vet Med* **19**, 8–18.

**Harrisson F and Callebaut M** (1993). Smooth muscle cells in the peritubular tissue of the quail testis. *Eur J Morphol* **31**, 60–4.

**Hasirci E, Turunc T, Bal N, Goren MR, Celik H, Kervancioglu E, Dirim A, Tekindal MA and Ozkardes H** (2017). Distribution and number of Cajal-like cells in testis tissue with azoospermia. *Kaohsiung J Med Sci* **33**, 181–6.

**Holdcraft RW and Braun RE** (2004). Androgen receptor function is required in Sertoli cells for the terminal differentiation of haploid spermatids. *Development* **131**, 459–67.

**Hsu SM, Raine L and Fanger HX** (1981). Use of avidin-biotin-peroxidase complex (ABC) in immunoperoxidase techniques: a comparison between ABC and unlabeled antibody (PAP) procedures. *J Histochem Cytochem* **29**, 577–80.

**Kannan TA, Venkatesan S and Geetha R** (2008). Histochemical studies on the testis of the Japanese quail. *Indian Vet J* **85**, 1129–30.

**Karnovsky MJ** (1965). A formaldehyde–glutaraldehyde fixative of high osmolarity for use in electron microscopy. *Cell Biol* **27**, 137–8A.

**Kimura N, Mizokami A, Oonuma T, Sasano H and Nagura H** (1993). Immunocytochemical localization of androgen receptor with polyclonal antibody in paraffin-embedded human tissues. *J Histochem Cytochem* **41**, 671–8.

**Kirby JD and Froman DP** (2000). Reproduction in male birds. In *Sturkie's Avian physiology*, 5th edn. (ed. CG Whittow). Academic Press, New York, pp. 597–615.

**Kormano M and Hovatta O** (1972). Contractility and histochemistry of the myoid cell layer of the rat seminiferous tubules during postnatal development. *Z Anat Entwicklungs* **137**, 239–48.

**Lan WEI, Peng KM, Liu H, Song H, Wang Y and Tang L** (2011). Histological examination of testicular cell development and apoptosis in the ostrich chick. *Turk J Vet Anim Sci* **35**, 7–14.

**Li X, Wang Z, Jiang Z, Guo J, Zhang Y, Li C, Chung J, Folmer J, Liu J, Lian Q, Ge R, Barry RZ and Ge R** (2016). Regulation of seminiferous tubule-associated stem Leydig cells in adult rat testes. *Proc Natl Acid Sci USA* **113**, 2666–71.

**Lin M and Jones RC** (1992). Renewal and proliferation of spermatogonia during spermatogenesis in the Japanese quail, *Coturnix coturnix japonica*. *Cell Tissue Res* **267**, 591–601.

**Lin M and Jones RC** (1993). Spermiogenesis and spermiation in the Japanese quail (*Coturnix coturnix japonica*). *J Anat* **183**, 525.

**Madkour FA and Mohamed AA** (2019). Comparative anatomical studies on the glandular stomach of the rock pigeon (*Columba livia targia*) and the Egyptian laughing dove (*Streptopelia senegalensis aegyptiaca*). *Anat Histol Embryol* **48**, 53–63.

**Maekawa M, Kamimura K and Nagano T** (1996). Peritubular myoid cells in the testis: their structure and function. *Arch Histol Cytol* **59**, 1–13.

**Marini M, Rosa I, Guasti D, Gacci M, Sgambati E, Ibba-Manneschi L and Manetti M** (2018). Reappraising the microscopic anatomy of human testis: identification of telocyte networks in the peritubular and intertubular stromal space. *Sci Rep* **8**, 14780.

**Nicholls TJ and Graham GP** (1972). Observations on the ultrastructure and differentiation of Leydig cells in the testis of the Japanese quail (*Coturnix coturnix japonica*). *Biol Reprod* **6**, 179–92.

**Niedenberger BA, Cook K, Baena V, Serra ND, Velte EK, Agno JE, Litwa KA, Terasaki M, Hermann BP, Matzuk MM and Geyer CB** (2018). Dynamic cytoplasmic projections connect mammalian spermatogonia *in vivo*. *Development* **145**, 161323.

**Pawlicki P, Hejmej A, Milon A, Lustofin K, Płachno BJ, Tworzydlo W, Gorowska-Wojtowicz E, Pawlicka B, Kotula-Balak M and Bilinska B** (2019). Telocytes in the mouse testicular interstitium: implications of G-protein-coupled estrogen receptor (GPER) and estrogen-related receptor (ERR) in the regulation of mouse testicular interstitial cells. *Protoplasma* **256**, 393–408.

**Regadera J, MartÍnez-GarcÍa F, González-Peramato P, Serrano A, Nistal M and Suárez-Quian C** (2001). Androgen receptor expression in Sertoli cells as a function of seminiferous tubule maturation in the human cryptorchid testis. *J Clin Endocrinol Metab* **86**, 413–21.

**Reynolds ES** (1963). The use of lead citrate at high pH as an electron-opaque stain in electron microscopy. *J Cell Biol* **17**, 208.

**Rothwell B** (1973). The ultrastructure of Leydig cells in the testis of the domestic fowl. *J Anat* **116**, 245.

**Rothwell B and Tingari MD** (1973). The ultrastructure of the boundary tissue of the seminiferous tubule in the testis of the domestic fowl (*Gallus domesticus*). *J Anat* **114**, 321.

**Ruizeveld de Winter J, Trapman J, Vermey M, Mulder E, Zegers N and van der Kwast T** (1991). Androgen receptor expression in human tissues: an immunohistochemical study. *J Histochem Cytochem* **39**, 927–36.

**Scheltinga DM and Jamieson BG** (2003). Spermatogenesis and the mature spermatozoon: form, function and phylogenetic implications. In *Reproductive Biology and Phylogeny of Anura* (ed. BGM Jamieson). Science Publishers, Inc., pp. 119–251.

**Sharpe RM, McKinnell C, Kivlin C and Fisher JS** (2003). Proliferation and functional maturation of Sertoli cells, and their relevance to disorders of testis function in adulthood. *Reproduction* **125**, 769–84.

**Shi L, Xun W, Zhou H, Hou G, Yue W, Zhang C, Ren Y and Yang R** (2013). Ultrastructure of germ cells, Sertoli cells and mitochondria during spermatogenesis in mature testis of the Chinese Taihang black goats (*Capra hircus*). *Micron* **50**, 14–9.

**Sutinen P, Malinen M and Palvimo JJ** (2017). Androgen receptor. In *Endocrinology of the Testis and Male Reproduction* (eds M Simoni and I Huhtaniemi). Springer, pp. 395–416.

**Trefil P, Micáková A, Mucksová J, Hejnar J, Poplstein M, Bakst MR, Kalina J and Brillard JP** (2006). Restoration of spermatogenesis and male fertility by transplantation of dispersed testicular cells in the chicken. *Biol Reprod* **75**, 575–81.

**Ventela S, Toppari J and Parvinen M** (2003). Intercellular organelle traffic through cytoplasmic bridges in early spermatids of the rat: mechanisms of haploid gene product sharing. *Mol Biol Cell* **14**, 2768–80.

**Villagra LI, Ramos I, Cisint S, Crespo CA and Fernández SN** (2018). Electron microscopy observations on testis and spermatozoa of *Leptodactylus chaquensis* (Anura, Leptodactylidae). *Micron* **105**, 35–46.

**Vornberger W, Prins G, Musto N and Suarez-Quian C** (1994). Androgen receptor distribution in rat testis: new implications for androgen regulation of spermatogenesis. *Endocrinology* **134**, 2307–16.

**Yang P, Ahmad N, Hunag Y, Ullah S, Zhang Q, Waqas Y, Liu Y, Li Q, Hu L and Chen Q** (2015). Telocytes: novel interstitial cells present in the testis parenchyma of the Chinese soft-shelled turtle *Pelodiscus sinensis*. *J Cell Mol Med* **19**, 2888–99.

**Wang RS, Yeh S, Tzeng CR and Chang C** (2009). Androgen receptor roles in spermatogenesis and fertility: lessons from testicular cell-specific androgen receptor knockout mice. *Endocrine Rev* **30**, 119–32.

**Welsh M, Moffat L, Belling K, De Franca L R, Segatelli TM, Saunders PTK, Sharpe RM and Smith LB** (2012). Androgen receptor signalling in peritubular myoid cells is essential for normal differentiation and function of adult Leydig cells. *Int J Androl* **35**, 25–40.

**Wright WW and Frankel AI** (1980). An androgen receptor in the nuclei of late spermatids in testes of male rats. *Endocrinology* **107**, 314–8.

**Zhou X, Kudo A, Kawakami H and Hirano H** (1996). Immunohistochemical localization of androgen receptor in mouse testicular germ cells during fetal and postnatal development. *Anat Rec* **245**, 509–18.

**Zhu LJ, Hardy MP, Inigo IV, Huhtaniemi I, Bardin CW and Moo-Young AJ** (2000). Effects of androgen on androgen receptor expression in rat testicular and epididymal cells: a quantitative immunohistochemical study. *Biol Reprod* **63**, 368–76.